Nonlinear Dyn (2018) 94:679–692
https://doi.org/10.1007/s11071-018-4385-9

ORIGINAL PAPER

Elimination of spiral waves in excitable media by magnetic induction

Zahra Rostami · Sajad Jafari · Matjaž Perc · Mitja Slavinec

Received: 2 March 2018 / Accepted: 19 May 2018 / Published online: 1 June 2018

Abstract The formation of spiral waves in excitable media is a fascinating example of the beauty of nonlinear dynamics in spatiotemporal systems. Apart from the beauty of the patterns, the subject also has many practical application. For example, the emergence of spiral waves in cardiac tissue can lead to arrhythmias. Cortical spiral waves are also involved in epileptic seizures. Motivated by this, we here study the effects of magnetic induction on the formation of spiral waves in excitable media. An external sinusoidal magnetic induction with different amplitudes and angular frequencies is applied in order to study whether spiral waves could be eliminated. We use a network of coupled neurons as a model for the excitable medium. The four-variable magnetic Hindmarsh–Rose model is used for the local dynamics of each isolated neuron. The distribution of the cell membrane potential over time, affected by magnetic induction, is determined and the results are depicted as snapshots of the 2D network. Our research reveals that the continuance of rotating spiral seeds is impaired by high-amplitude magnetic induction. Moreover, we show that low-frequency induction is not capable of breaking the reorganizing rhythm of the spiral seeds, while much higher frequencies can be too fast to overcome this special rhythm.

Keywords Spiral wave · Spatiotemporal pattern · Magnetic flux · Neuronal network · Magnetic Hindmarsh–Rose model

Z. Rostami · S. Jafari
Biomedical Engineering Department, Amirkabir University of Technology, Tehran 15875-4413, Iran
e-mail: z.rostami.zrmi@gmail.com

S. Jafari
e-mail: sajadjafari83@gmail.com

M. Perc (✉) · M. Slavinec
Faculty of Natural Sciences and Mathematics, University of Maribor, Koroška cesta 160, 2000 Maribor, Slovenia
e-mail: matjaz.perc@uni-mb.si

M. Slavinec
e-mail: mitja.slavinec@um.si

M. Perc
CAMTP – Center for Applied Mathematics and Theoretical Physics, University of Maribor, Mladinska 3, 2000 Maribor, Slovenia

M. Perc
Complexity Science Hub, Josefstädterstraße 39, 1080 Vienna, Austria

1 Introduction

Neuronal system is a complex system that exhibits collective behaviors. Collective behavior is one of the most dominant characteristics of complex systems and cannot simply be inferred from the properties of the individual components [1–3]. More detailed definitions of the complexity and the complex systems can be found in Ref. [4]. Neuronal network, an assembly of a large number of neurons interacting with each other [5,6], is capable of representing complex demonstrations [7]. These complexities can be in the form of synchronized or asynchronized behaviors, which are the important properties of the dynamical networks [8]. They are also

useful to understand some other behaviors of such systems including the self-organized behaviors [9]. Actually, studying neuronal network helps us understand some possible collective behaviors and some mechanisms of biological systems [10], and then it enables us explain some biological experiments [11]. Generally, network science has brought a valuable point of view for investigation of the functional and structural properties of different physical, chemical, technological and biological systems [12]. As a fact, understanding the dynamics of the biological systems in health or disease condition has proved to be a challenging problem from different aspects of their anatomical, physiological and physical properties. It is important to improve the treatments and therapeutic methods based on the theoretical studies and clinical experiments. Therefore, many experts and researchers have focused on this issue to obtain beneficial perception of the laws that govern these systems. In this regard, mathematical modeling has proved to be useful to get closer to the basics of the dynamics of such systems [12].

Fundamentally, the mechanism of wave propagation as a spatiotemporal behavior is the most efficient tool to characterize the neuronal network. It is confirmed that formation of spatiotemporal pattern is a phenomenon that exists in the systems with locally active elements [13]. In addition, pattern formation is one of the main problems in different fields of science, specially in complex nonlinear systems [14]. There can be found more conceptual definitions and useful guidance for pattern formation and pattern selection and their application in collective response of neuronal networks in Ref. [15]. Having a close relationship with the dynamics of an excitable system, spatiotemporal patterns have attracted much attention. For instance, Mvogo et al. [16] addressed the nonlinear patterns in an excitable media with the consideration of magnetic flux effects. Takembo et al. [17] analyzed the onset of modulated waves in a model of myocardial cell excitations. In some cases, the propagating wave takes place in a specific pattern, which may be known for its special properties.

Spiral wave is a unique self-organized and self-sustained pattern. The dynamics of the spiral wave is basically determined by its center (seed). As soon as a spiral seed emerges in the tissue, the spiral wave starts to travel along expanding circular paths with some particular properties and capabilities. The first simulation of the spiral wave was introduced in 1972 for a reduced system of Hodgkin–Huxley (HH) model [13]. Spiral waves are also investigated by a number of discrete or continuous form of mathematical models [19]. Zhang et al. [20] investigated the spiral tip trajectory in the cardiac tissue model. Banerjee et al. [21] discussed the circumstances in which the spiral waves emerge in a prey–predator model. Woo et al. [22] employed the sine-circle map for their numerical analysis of coupled nonlinear oscillators forming a two-dimensional network. Hu et al. [23] studied the multi-armed spiral waves in a regular network of HH neurons. Li et al. [24] obtained spiral pattern from the collective behaviors of a network of improved Chua oscillators. Perc discussed the effect of small-world connectivity on the spatial patterns including spiral patterns in a neural media [25]. Panfilov et al. [26] studied the elimination of spiral wave in cardiac tissue using multiple electrical shocks.

Considering the biological applications, spiral pattern relies on recurrent excitations or reentrant waves in an excitable media [27–29] (e.g., cardiac media or brain tissue). The statistics show that reentry is known as the most prominent type of abnormal heart rhythms [30]. It is believed that one of the mechanisms that give rise to the heart arrhythmias is two-dimensional spiral waves or three-dimensional spiral (scroll) waves [28,29]. In fact, emergence of the spiral waves makes the heart constrict more frequently. As a spiral seed breaks up into multiple seeds, the constriction of the heart muscle fibers becomes spontaneously asynchronized and rapid. This state is known as fibrillation [31], which prevents the heart from pumping the oxygenated blood to the body. This is the leading reason of morality, resulting in a large number of deaths each year [30]. Some theoretical studies or experimental strategies like pacing or electrical shocks are used to control these arrhythmias.

Furthermore, reported observations affirm the emergence of the spiral waves in slices of the cortical tissue [18,32,33]. Although, it is confirmed that spiral pattern is essential for a number of ongoing cortical activities [18], it plays an effective role in some brain abnormalities and failures, as well. Some experimental results denote that the epileptiform bursts can organize into spiral demonstrations [32], which means that cortical spiral waves can be involved in epileptic seizures [34]. There has also introduced a method to detect the spiral activity in cortical models of epilepsy [32].

Substantially, the dynamics of a real neuron is so complicated while it is governed by various internal

and external factors. For example, based on the electromagnetic induction theorem, the fluctuation of the neuron's membrane potential can change the intracellular and extra-cellular electromagnetic field [35]. In fact, the internal electromagnetic field in the body plays an essential role in some biochemical reactions. Besides, the external electromagnetic field significantly influences the neuron's electrical response, as well [36]. Therefore, some efforts are taken to improve the mathematical models that are known for their similar demonstrations to the real neuron's behavior. Some researchers propose new models, in which the effect of magnetic flux is included [10,37,38]. This magnetic flux describes the effects of time-varying electromagnetic field, which is caused by the ion currents across the membrane and the fluctuations of ion concentration inside and outside of the cell body [39].

Recently, the effect of magnetic stimulation on the neurons and their electrical behavior is extensively noticed. Magnetic stimulation is a non-invasive and painless technique, in which the neurons are induced by a magnetic signal, which can be in a sinusoidal form [40]. The generated magnetic field can induce an electric field and depolarize the neurons [41], so that the neurons are activated. This method is also known as a modulating operation for therapy applications [41]. It is interesting to study the effect of magnetic induction on the spatiotemporal representation of a neuronal network. Since the collective behavior of neuronal network basically comes from the aggregation of the dynamics of the individual neurons, it is worth applying the required improvements to the mathematical model of an isolated neuron. In this study, we use a new neuronal model in which the magnetic flux is considered. Besides, we define a parameter for the external magnetic induction. The results show that the spiral seeds can be suppressed by the effect of magnetic induction. In fact, in a neuronal network, as a model of an excitable tissue, both the amplitude and the angular frequency of the magnetic radiation have their own influences on maintenance or elimination of the spiral seed. Combining these two factors can bring the tissue different spatial and temporal behaviors. We aim to track the changes of these behaviors under different intensities of the magnetic induction. Therefore, some different amplitudes and frequencies are applied and the results are well sorted to be compared more easily.

For the rest of the paper, we explain the mathematical model used for our simulations in Sect. 2. The results of our computational modeling are represented in Sect 3. Besides, the detailed descriptions of the spatiotemporal electrical activities obtained under different circumstances are given in this section as well. For the last, the conclusion of this paper can be found in Sect. 4.

2 Model and description

The Hindmarsh–Rose (HR) neuronal model [42] is a reduced form of Hodgkin–Huxley (HH) neuronal model [43]. The HR model is mostly known for the spiking–bursting dynamics, which is the alternation between high and low activities [44]. As mentioned above, regarding the reality of the dynamics of a neuron, it is necessary to consider the real neuronal structure and its physical condition to obtain a more reliable model for the investigations. Therefore, the new neuronal model is proposed with the magnetic flux being considered. In this four dimensional model, the fourth variable shows the magnetic flux describing the effect of the time-varying electromagnetic field. Moreover, a memristive coupling is considered between the membrane potential and the magnetic flux [45]. The local dynamics of an isolated neuron is described as follows:

$$\begin{aligned}
\frac{\mathrm{d}x}{\mathrm{d}t} &= y - ax^3 + bx^2 - z + I_{\mathrm{ex}} - k_1 w(\phi)x \\
\frac{\mathrm{d}y}{\mathrm{d}t} &= c - \mathrm{d}x^2 - y \\
\frac{\mathrm{d}z}{\mathrm{d}t} &= r(s(x - x_0) - z) \\
\frac{\mathrm{d}\phi}{\mathrm{d}t} &= x - k_2\phi + \phi_{\mathrm{ex}} \qquad (1) \\
w(\phi) &= \alpha + 3\beta\phi^2 \qquad (2)
\end{aligned}$$

where the variables x, y, z, ϕ represent the membrane potential, the slow current for recovery variable, the adaptation current and the magnetic flux across the membrane, respectively. The parameters $k_1 = 1$ and $k_2 = 0.5$ denote the interaction between magnetic flux and membrane potential [45]. w is a function of magnetic flux introducing the conductance of memristor [46]. Memristor is a two-terminal nonlinear circuit element that connects the two fundamental circuit variables charge and flux [47]. The existence of this element is also showed by Hewlett–Packard (HP) laboratory [48], experimentally [49]. In Eq. 2, $\alpha = 0.1$ and $\beta = 0.02$ are fixed parameters. We set $a = 1$, $b = 3$,

$c = 1, d = 5, s = 4, r = 0.006, x_0 = -1.6$. ϕ_{ex} is the external magnetic radiation and I_{ex} is the external current force. In the HR model, the level of I_{ex} determines the state of a HR neuron including quiescent, spiking, bursting or even chaotic behaviors. In this paper, we choose $I_{\text{ex}} = 2.8$, which is supposed to bring the individual neuron spiking state [45]. However, this individual neuron is capable of representing other behaviors due to interaction with other neighbor neurons. For example, the numerical simulations show that bursting behavior can be deduced from a spiking neuron as well as a fast spiking neuron while connecting to some other neurons in a neuronal network. The fast spike is a type of action potential generation initiated in axon initial segment [50] and is followed by back propagation into the apical dendrite [51]. Because of the network template we follow in this paper, it is better to mention parameter I_{ex} as the level of excitability of the whole network.

In Eq. 1, the term $k_1 w(\phi)x$ is based on Faraday law of electromagnetic induction and is described as follow:

$$i = \frac{\mathrm{d}q(\phi)}{\mathrm{d}t} = \frac{\mathrm{d}q(\phi)}{\mathrm{d}\phi}\frac{\mathrm{d}\phi}{\mathrm{d}t} = w(\phi)V = k_1 w(\phi)x \qquad (3)$$

where V denotes the electromotive force and k_1 shows the feedback gain [42].

For the purpose of designing a two-dimensional square network, we rewrite Eqs. 1 and 2 as follows:

$$\begin{aligned}
\frac{\mathrm{d}x_{ij}}{\mathrm{d}t} &= y_{ij} - ax_{ij}^3 + bx_{ij}^2 - z_{ij} + I_{\text{ex}} - k_1 w(\phi_{ij})x_{ij} \\
&\quad + G(x_{i+1j} + x_{i-1j} + x_{ij+1} + x_{ij-1} - 4x_{ij}) \\
&\quad + f\sigma_{i\theta}\sigma_{j\gamma} \\
\frac{\mathrm{d}y_{ij}}{\mathrm{d}t} &= c - \mathrm{d}x_{ij}^2 - y_{ij} \\
\frac{\mathrm{d}z_{ij}}{\mathrm{d}t} &= r(s(x_{ij} - x_0) - z_{ij}) \\
\frac{\mathrm{d}\phi_{ij}}{\mathrm{d}t} &= x_{ij} - k_2\phi_{ij} + \phi_{\text{ex}}\delta_{i\eta}\delta_{j\zeta} \qquad (4) \\
w(\phi_{ij}) &= \alpha + 3\beta\phi_{ij}^2 \qquad (5)
\end{aligned}$$

where the subscript ij shows the position of each neuron in the two-dimensional network. Equations 4 and 5 represent a one-layer network, in which each neuron is coupled with its four-neighbor neurons. Parameter $G = 1$ is a constant coupling intensity between the neurons and indicates the diffusion coefficient. f is a momentary force only to trigger the wave. $\sigma_{i\theta} = 1$ for $i = \theta, \sigma_{i\theta} = 0$ for $i \neq \theta; \sigma_{j\gamma} = 1$ for $j = \gamma, \sigma_{j\gamma} = 0$ for $j \neq \gamma$. We impose f on the central part of the network by setting $\gamma = \theta = 50$. As the same way, $\delta_{i\eta} = 1$ for $i = \eta, \delta_{i\eta} = 0$ for $i \neq \eta; \delta_{j\zeta} = 1$ for $j = \zeta$, $\delta_{j\zeta} = 0$ for $j \neq \zeta$. We can choose the region to which the external magnetic flux (ϕ_{ex}) is induced by adjusting the parameters η and ζ. Besides, ϕ_{ex} consists of ϕ_{ex}^1 and ϕ_{ex}^2 (the exact coordinates of ϕ_{ex}^1 and ϕ_{ex}^2 are given in the following). We set $\eta = 20:47$ and $\zeta = 20:47$, $\eta = 53:80$ and $\zeta = 53:80$ for ϕ_{ex}^1; $\eta = 20:47$ and $\zeta = 53:80$, $\eta = 53:80$ and $\zeta = 20:47$ for ϕ_{ex}^2. To put it clear, the area that is exposed to the external magnetic induction is illustrated in Fig. 1. We apply the sinusoidal external magnetic induction by $\phi_{\text{ex}}^1 = A_1 \sin(\omega t)$ in the first two square-shaped areas and $\phi_{\text{ex}}^2 = A_2 \sin(\omega t)$ in the second two square-shaped areas (see Fig. 1) from $t = 1500$ to $t = 2000$ time units. For more illustration, the area of the excitable media exposed to the external magnetic induction is depicted in Fig. 1.

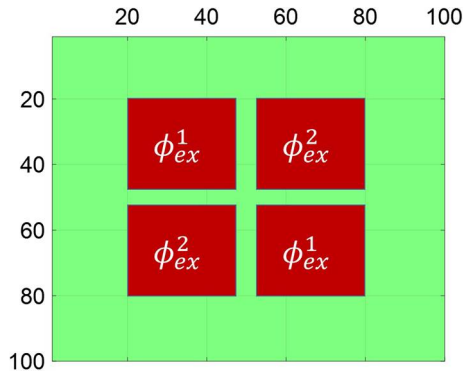

Fig. 1 The area of the excitable media exposed to the external magnetic induction. $\phi_{\text{ex}}^1 = A_1 \sin(\omega t)$ is the external magnetic induction applied to the first two square-shaped areas; $\phi_{\text{ex}}^2 = A_2 \sin(\omega t)$ is the external magnetic induction applied to the second two square-shaped areas

3 Numerical analysis and discussion

In this section, we discuss our numerical method and the simulation results. We design a square network consists of 100×100 neurons and no flux boundary condition is considered. The fourth-order Runge–Kutta algorithm is used for the numerical study with time step $h = 0.01$. The initial states of the variables are $(x, y, z, \phi) = (0.01\ \ 0.02\ \ 0.003\ \ 1.01)$. The distribution of the membrane potential in both time domain and space domain is detected and some snapshots of the resulting evolutionary patterns are displayed. By aim-

ing to see the effect of magnetic induction on the spiral waves in an excitable tissue, we need to trigger a wave front leading to formation of spiral waves for our simulation. Therefore, the parameters are adjusted in a way that spiral seeds find emergence. We impose a current force to the center of the tissue for initiation of the wave front. The circular traveling wave fronts get into four symmetrical paired spirals, which are emerged under appropriate adjustments. The evolution of the expanding wave front and formation of the spiral seeds are shown in Fig. 2.

Since the dynamics of spiral wave is determined by its central part known as the spiral seed, we apply different intensities of external magnetic induction to the spiral seeds in four limited areas, specified in the previous section (Fig. 1). In this way, the maintenance or suppression of the existed spiral waves under magnetic induction can be investigated. We apply six angular frequencies and six levels of amplitude for each frequency, and then put the results in a well comparable order. The results confirm that continuance of rotating spiral seeds suffer from higher amplitude. Also increasing the frequency (parameter ω) up to a certain threshold restricts maintenance of spiral seed. However, it should be mentioned that too much increase in frequency is not suitable for suppression of the spiral waves while the low frequencies are not capable of breaking the reorganizing rhythm of the spiral seeds.

Firstly, we set $\omega = 0.001$ with different amplitudes of $0.5, 1, 1.5, 2, 2.5, 3$. Figure 3 shows the results within five snapshots over the time. In Fig. 3a–e, the amplitudes are set as $A_1 = 1$ and $A_2 = 0.5$. As is clear through these snapshots, the greater amplitude brings the spiral more restriction and the respective spirals (in the first two areas) become limited more (see Fig. 3e). Furthermore, we set $A_1 = 2$, $A_2 = 1.5$ for Fig. 3f–j and $A_1 = 3$, $A_2 = 2.5$ for Fig. 3k–o, respectively. Figure 3f–j shows a limited development of the spiral seeds. Besides, as is clear through the snapshots of Fig. 3k–o, further increase in the amplitude benefits eradication of the spiral seeds. However, this annihilation is at the expense of some other spiral seeds to emerge. In fact, very high amplitude causes a significant energy difference at the borders of the induction regions leading to such an imbalance that potentially provides favorable condition for formation of the secondary spiral seeds. This imbalance will come under control by the help of higher frequency that is explained in more details in the next few paragraphs. Here for this case, the secondary spiral seeds start to grow near the boundaries of the induction region, so that the secondary spiral waves are observable in Fig. 3o.

For the second, we apply a higher frequency by $\omega = 0.005$ and the six amplitude levels just as before. This little increase in frequency accompanied by amplitude of 1 as shown in Fig. 4a–e ($A_1 = 1$) confines the respective spirals from development (notice Fig. 4e). For $A_1 = 2$ and $A_2 = 1.5$ (Fig. 4f–j) all the spirals become broken, but then the secondary spiral seeds exist and start to get to the power for their continuous rotation. Figure 4h shows the moment in which the primary paired spirals are eliminated and existence of the secondary paired spirals are visible in Fig. 4i, j. By further increase in the amplitude (Fig. 4k–o), the primary paired spirals completely get annihilated even sooner than the previous ones. In this case, it is close that the secondary spiral seeds emerge. However, the recurrent excitations of the surface overcome the rhythm of these secondary seeds before they get to power (Fig. 4m–o). Actually, in general, the spiral seeds require a minimum power for the beginning of their existence to access a firm rotation.

For the next, we fix $\omega = 0.01$. As is clear in Fig. 5a–e, the amplitude of 1 ($A_1 = 1$) significantly restricts the respective paired spirals (see Fig. 5e). Here in this frequency, the increase in the amplitude does not cause emergence of the secondary spiral seeds. It seems that this level of frequency brings the borders of the induction regions a kind of balance and the energy difference at the borders caused by the amplitude difference is compensated to some extent (Fig. 5f–o). Consequently, there is no sign of any spiral activity in the final results displayed in Fig. 5j, o.

Moreover, Figs. 6 and 7 confirm that an appropriate angular frequency can eliminate the spiral seeds on its own and does not necessarily depend on the amplitude of the stimulus (see the final results depicted in Figs. 6e, j, o and 7e, j, o). More precisely, by this adjustment of $\omega = 0.05$ and $\omega = 0.1$, the elimination of the spiral seeds gets very soon and no secondary spiral seeds find opportunity to appear. Although, a higher amplitude was capable to supply the secondary seeds appear near the boundary of the induction regions for $\omega = 0.001$ and $\omega = 0.005$, for this case the parameters $\omega = 0.05$ and $\omega = 0.1$ balance the areas prone to seeds formation and make the tissue resist initiation of the secondary spiral seeds. A particular characteristic of the spiral seed is its high-frequency rotation relying

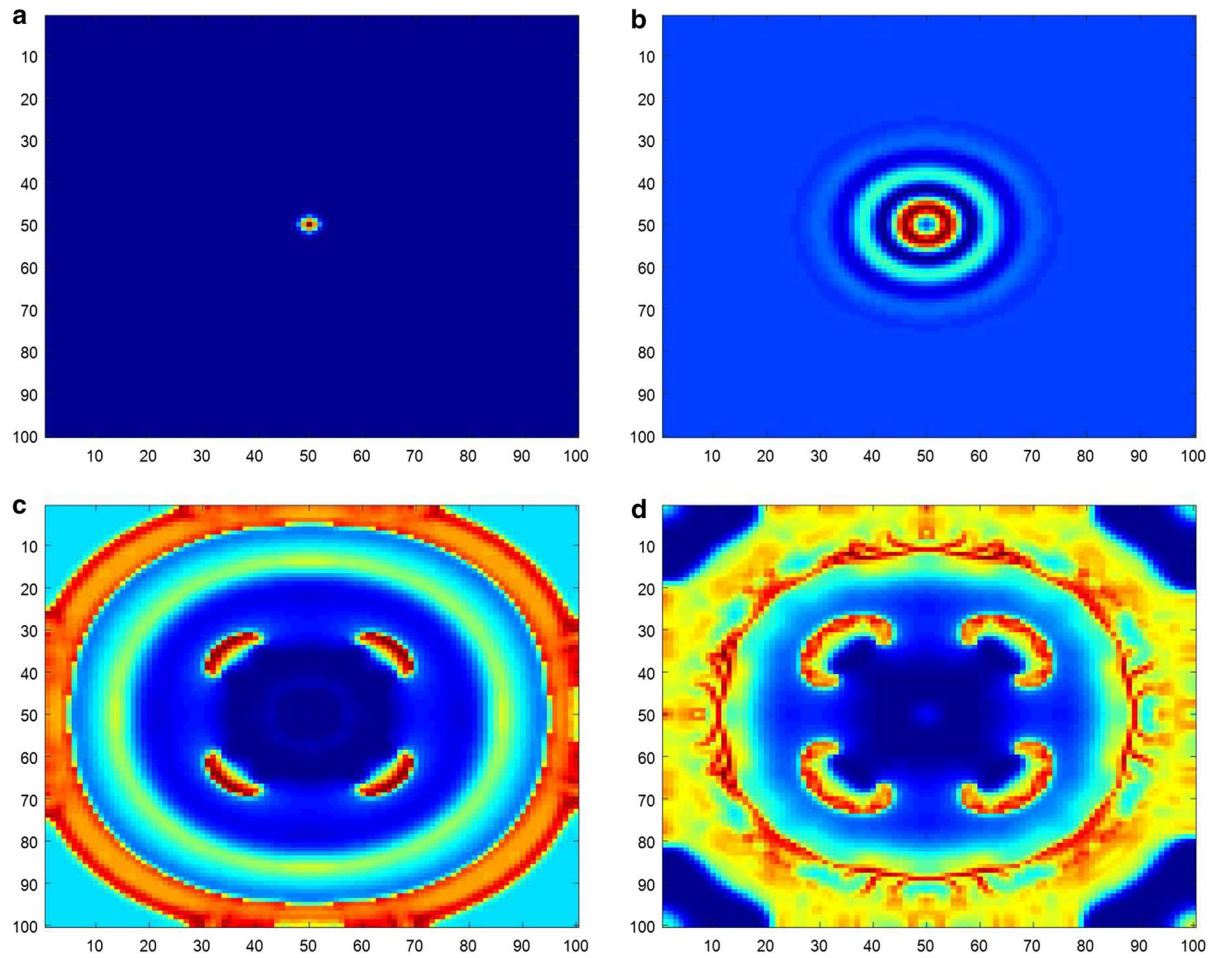

Fig. 2 The distribution of the membrane potential showing the evolution of expanding wave fronts and formation of the paired spirals; for **a** $t = 5$ time units, **b** $t = 350$ time units, **c** $t = 750$ time units, **d** $t = 1495$ time units

on the rhythm of the recurrent excitations. Actually, the recurrent excitations of the area, in which the spiral seed emerges, are faster than the other parts and also appear in a specific rhythm (spiral rhythm). Accordingly, the beneficial effect of the mentioned appropriate angular frequencies, by which the seeds were completely annihilated, may be related to this fact about spiral seeds characteristic.

Due to the results achieved so far, is it true that the higher angular frequency, the more destruction is brought for the spiral seed? To discover the answer of this question, we increase the frequency by $\omega = 0.5$ and show the results in Fig. 8. The results represented in Fig. 8 confirm that, too much increase in the angular frequency does not benefit elimination of the spiral seed. Figure 8a–j shows the evolution of the paired spiral waves under the angular frequency of $\omega = 0.5$ and the amplitudes of $A_1 = 1$, $A_2 = 0.5$, $A_1 = 2$, $A_2 = 1.5$. These results confirm that the primary paired spirals continue to rotate with no annihilation while the spiral area is exposed to a high-frequency magnetic stimulation (Fig. 8e, j). However, thanks to the higher amplitude the spirals represented in Fig. 8k–o cannot be sustained so they get vanished (Fig. 8o). Moreover, there is also no sign of secondary spiral seeds in this case that was observed in some of the previous cases. This is because of the increased frequency and the rendered balance near the magnetic stimulation borders.

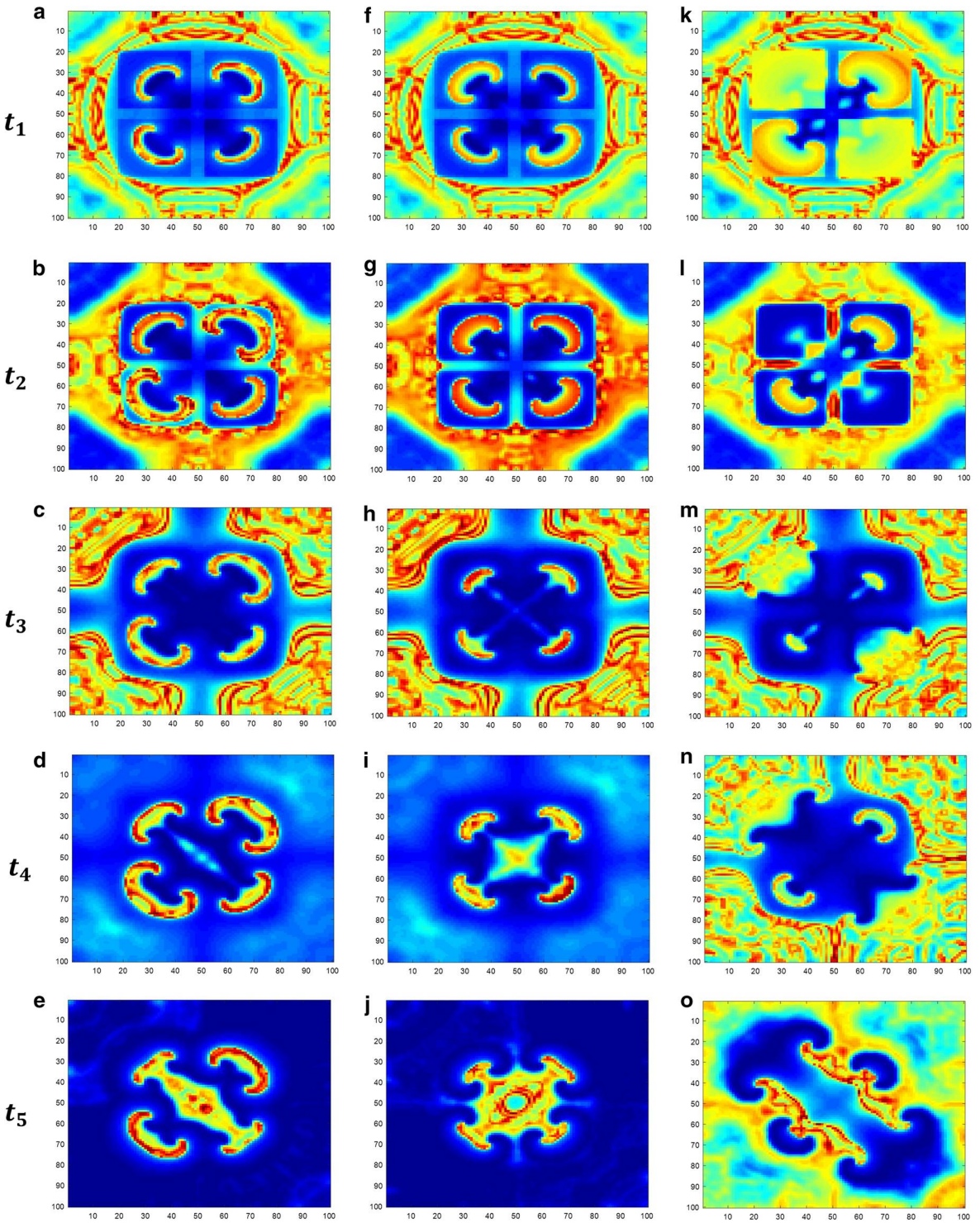

Fig. 3 The distribution of the membrane potential over the time, showing the effect of magnetic induction on the four square areas, in which the paired spirals exist, for $\omega = 0.001$, $t_1 = 1555$ time units, $t_2 = 1855$ time units, $t_3 = 2240$ time units, $t_4 = 2630$ time units, $t_5 = 3000$ time units. For **a**–**e** $A_1 = 1$, $A_2 = 0.5$, **f**–**j** $A_1 = 2$, $A_2 = 1.5$, **k**–**o** $A_1 = 3$, $A_2 = 2.5$. The magnetic induction starts from 1500 time units until 2000 time units

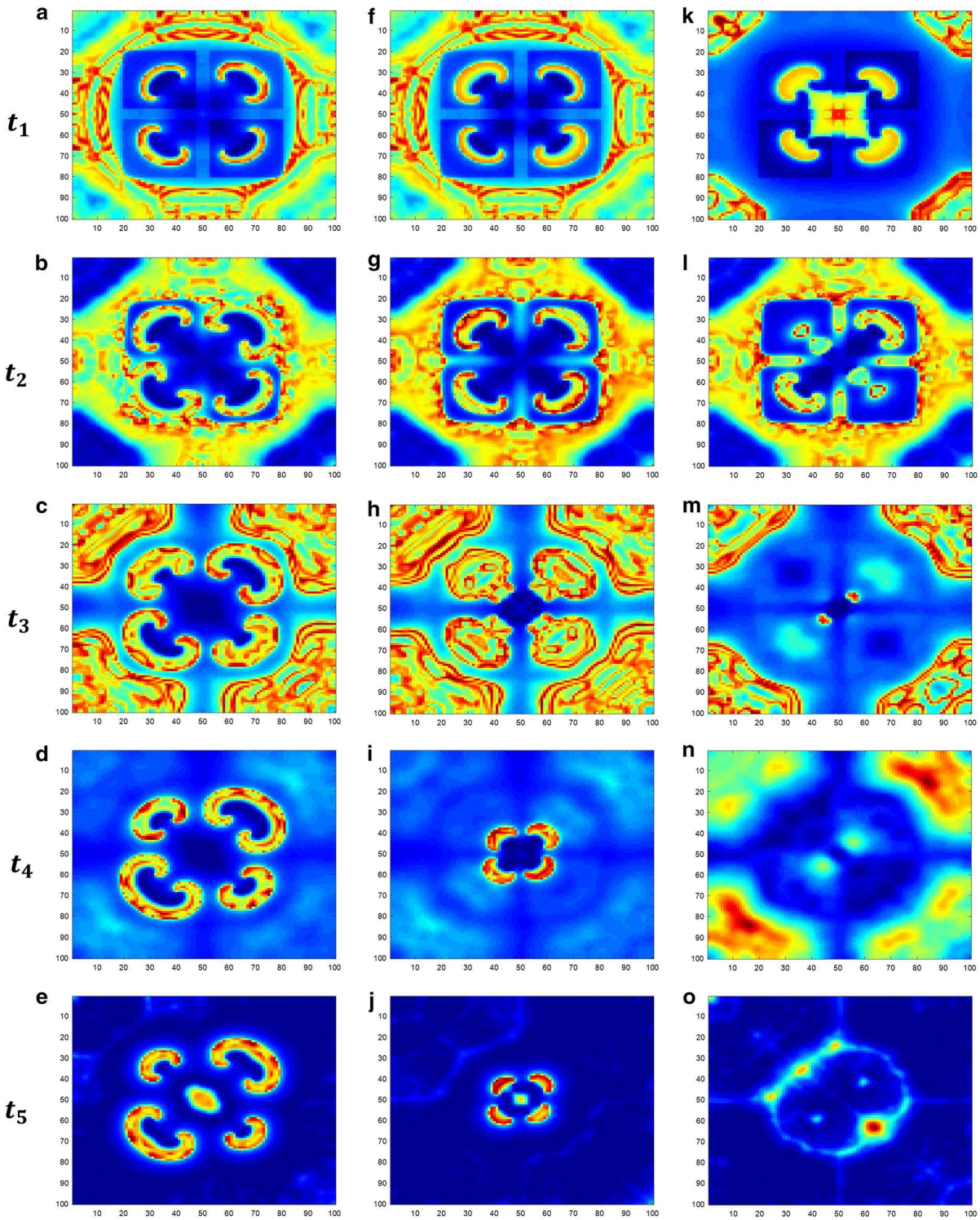

Fig. 4 The distribution of the membrane potential over the time, showing the effect of magnetic induction on the four square areas, in which the paired spirals exist, for $\omega = 0.005$, $t_1 = 1555$ time units, $t_2 = 1855$ time units, $t_3 = 2240$ time units, $t_4 = 2630$ time units, $t_5 = 3000$ time units. For **a**–**e** $A_1 = 1$, $A_2 = 0.5$, **f**–**j** $A_1 = 2$, $A_2 = 1.5$, **k**–**o** $A_1 = 3$, $A_2 = 2.5$. The magnetic induction starts from 1500 time units until 2000 time units

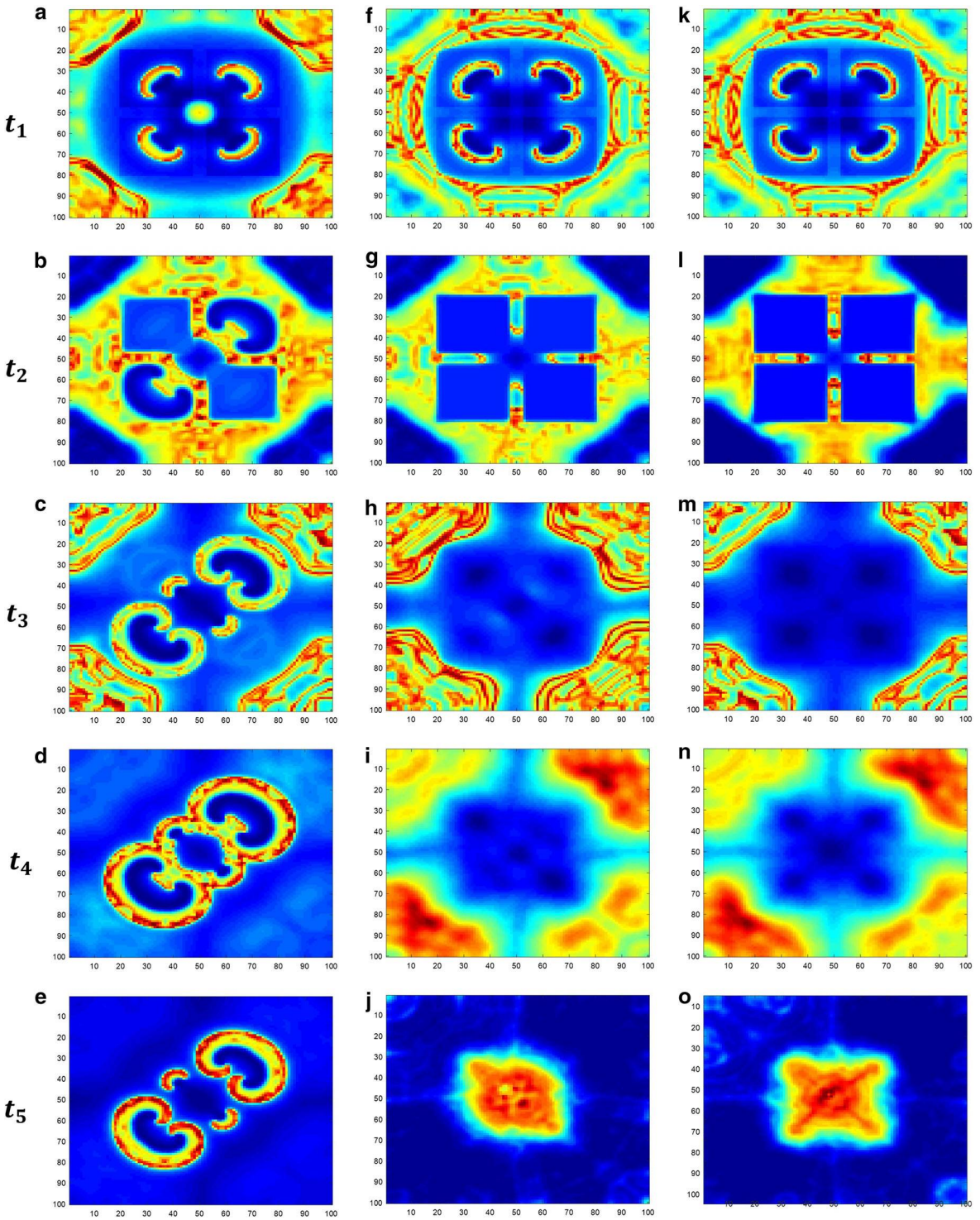

Fig. 5 The distribution of the membrane potential over the time, showing the effect of magnetic induction on the four square areas, in which the paired spirals exist, for $\omega = 0.01$, $t_1 = 1555$ time units, $t_2 = 1855$ time units, $t_3 = 2240$ time units, $t_4 = 2630$ time units, $t_5 = 3000$ time units. For **a**–**e** $A_1 = 1$, $A_2 = 0.5$, **f**–**j** $A_1 = 2$, $A_2 = 1.5$, **k**–**o** $A_1 = 3$, $A_2 = 2.5$. The magnetic induction starts from 1500 time units until 2000 time units

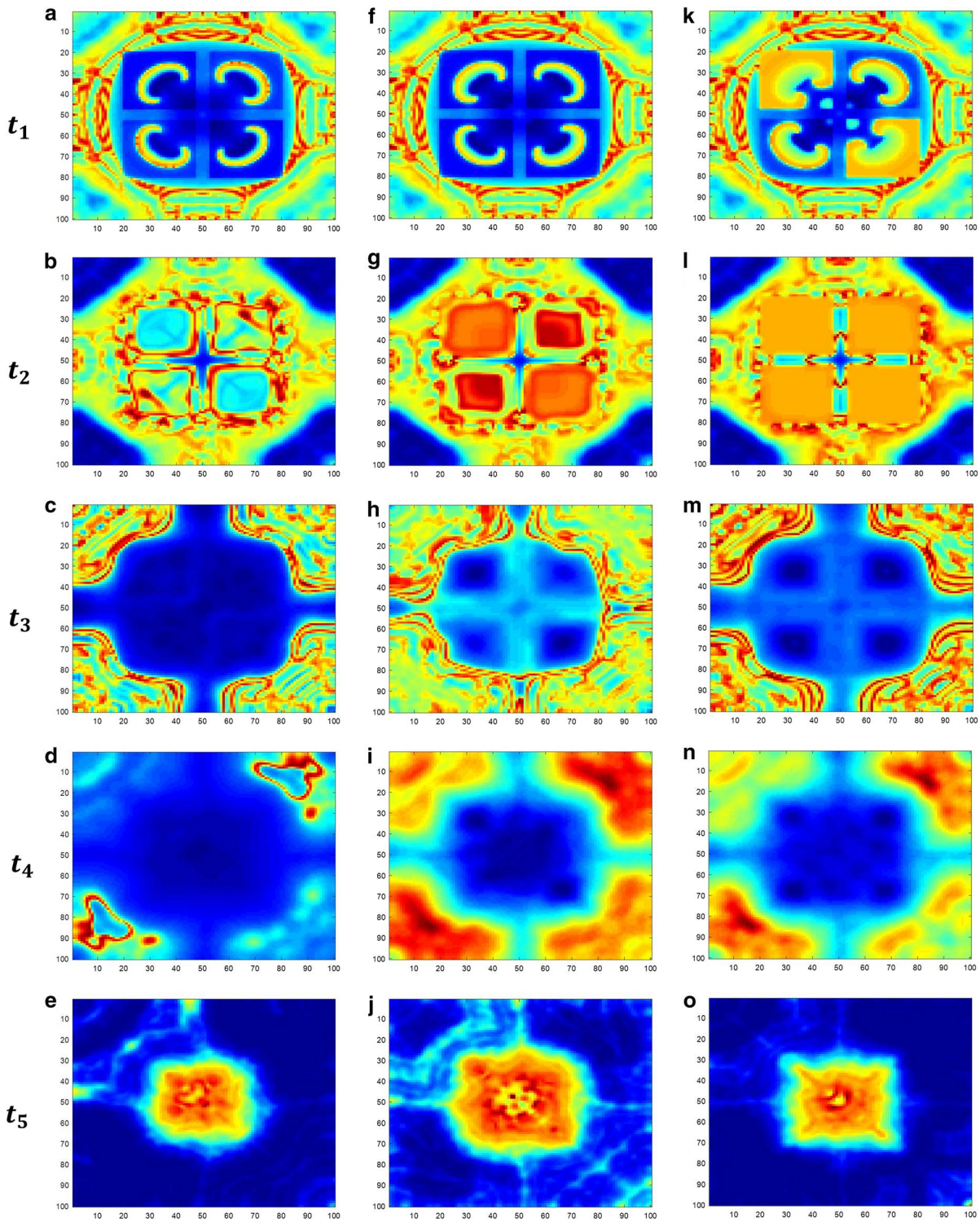

Fig. 6 The distribution of the membrane potential over the time, showing the effect of magnetic induction on the four square areas, in which the paired spirals exist, for $\omega = 0.05$, $t_1 = 1555$ time units, $t_2 = 1855$ time units, $t_3 = 2240$ time units, $t_4 = 2630$ time units, $t_5 = 3000$ time units. For **a**–**e** $A_1 = 1$, $A_2 = 0.5$, **f**–**j** $A_1 = 2$, $A_2 = 1.5$, **k**–**o** $A_1 = 3$, $A_2 = 2.5$. The magnetic induction starts from 1500 time units until 2000 time units

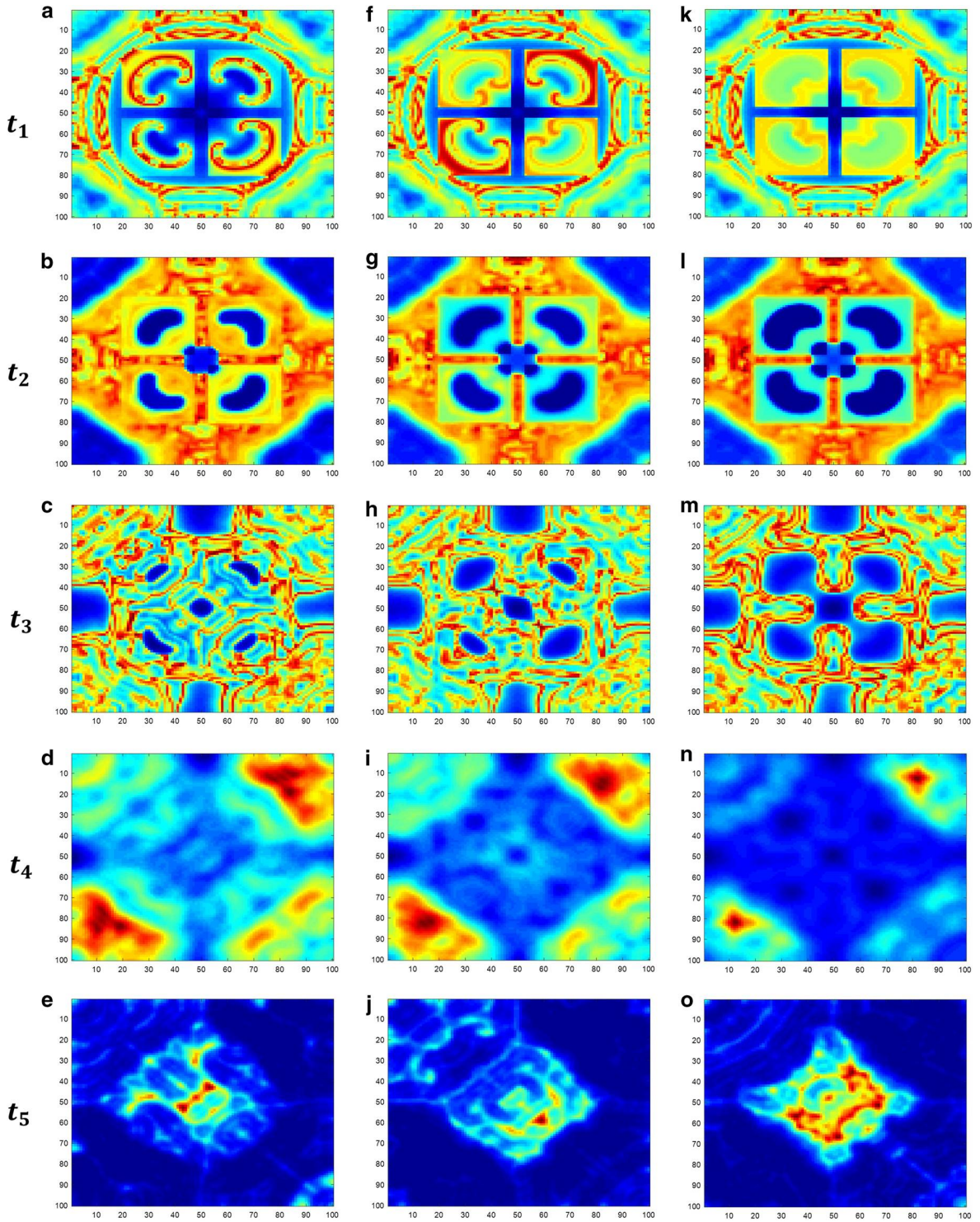

Fig. 7 The distribution of the membrane potential over the time, showing the effect of magnetic induction on the four square areas, in which the paired spirals exist, for $\omega = 0.1$, $t_1 = 1555$ time units, $t_2 = 1855$ time units, $t_3 = 2240$ time units, $t_4 = 2630$ time units, $t_5 = 3000$ time units. For **a**–**e** $A_1 = 1$, $A_2 = 0.5$, **f**–**j** $A_1 = 2$, $A_2 = 1.5$, **k**–**o** $A_1 = 3$, $A_2 = 2.5$. The magnetic induction starts from 1500 time units until 2000 time units

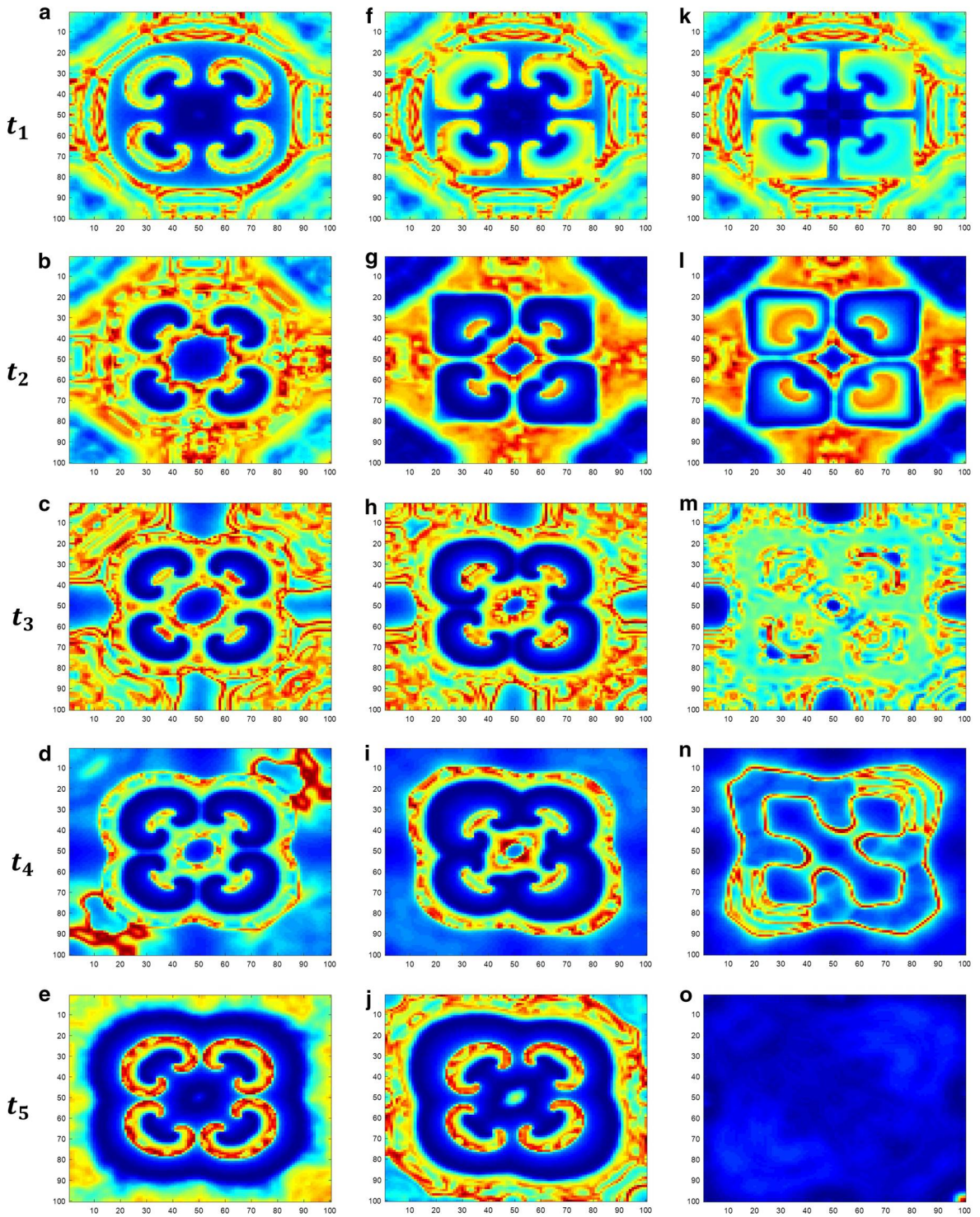

Fig. 8 The distribution of the membrane potential over the time, showing the effect of magnetic induction on the four square areas, in which the paired spirals exist, for $\omega = 0.5$, $t_1 = 1555$ time units, $t_2 = 1855$ time units, $t_3 = 2240$ time units, $t_4 = 2630$ time units, $t_5 = 3000$ time units. For **a**–**e** $A_1 = 1$, $A_2 = 0.5$, **f**–**j** $A_1 = 2$, $A_2 = 1.5$, **k**–**o** $A_1 = 3$, $A_2 = 2.5$. The magnetic induction starts from 1500 time units until 2000 time units

4 Conclusion

In this study, the effect of magnetic induction on the spiral waves emerged in an excitable media was investigated by computational modeling. For modeling an excitable media, a network of coupled neurons was designed, in which the local dynamic of each neuron was governed by the four-variable Hindmarsh–Rose neuronal model. The strong point of this new model is its property of being more reliable based on nonlinear dynamics of a real neuron. Actually, in this model, the time-varying magnetic field is considered, which is relied on the exchange of ions across the membrane and the resulting mutual effects of electrical field and magnetic field. An external sinusoidal magnetic induction was induced to the existed spiral seeds within different amplitudes and angular frequencies. So that the elimination of the spiral seeds under magnetic induction was investigated.

The results show that continuance of rotating spiral seeds suffers from high amplitude. Also increasing the angular frequency up to a threshold restricts maintenance of spiral seed. However, on the other hand, excessive increase in the angular frequency, as well as very low angular frequency, is not suitable for suppression of the spiral waves. In fact, low frequencies are not capable of breaking the reorganizing rhythm of the spiral seeds, while the excessive increased frequencies are too fast to overcome this particular spiral rhythm.

Acknowledgements Sajad Jafari was supported by the Iran National Science Foundation (Grant No. 96000815). Matjaž Perc was supported by the Slovenian Research Agency (Grants Nos. J1-7009 and P5-0027).

Compliance with ethical standards

Conflict of interest The authors declare that they have no conflict of interest.

References

1. Goldenfeld, N., Kadanoff, L.P.: Simple lessons from complexity. Science **284**, 87–89 (1999)
2. Gell-Mann, M.: Simplicity and complexity in the description of nature. Eng. Sci. **51**, 2–9 (1988)
3. Perc, M.: Stability of subsystem solutions in agent-based models. Eur. J. Phys. **39**, 014001 (2017)
4. Holovatch, Y., Kenna, R., Thurner, S.: Complex systems: physics beyond physics. Eur. J. Phys. **38**(2), 023002 (2017)
5. Guo, S., Xu, Y., Wang, C., Jin, W., Hobiny, A., Ma, J.: Collective response, synapse coupling and field coupling in neuronal network. Chaos Solitons Fractals **105**, 120–127 (2017)
6. Wu, F., Wang, Y., Ma, J., Jin, W., Hobiny, A.: Multi-channels coupling-induced pattern transition in a tri-layer neuronal network. Physica A **493**, 54–68 (2018)
7. Yilmaz, E., Ozer, M., Baysal, V., Perc, M.: Autapse-induced multiple coherence resonance in single neurons and neuronal networks. Sci. Rep. **6**, 30914 (2016)
8. Li, X., Rakkiyappan, R., Sakthivel, N.: Non-fragile synchronization control for markovian jumping complex dynamical networks with probabilistic time-varying coupling delays. Asian J. Control **17**, 1678–1695 (2015)
9. Li, X., Fu, X.: Synchronization of chaotic delayed neural networks with impulsive and stochastic perturbations. Commun. Nonlinear Sci. Numer. Simul. **16**, 885–894 (2011)
10. Ma, J., Tang, J.: A review for dynamics in neuron and neuronal network. Nonlinear Dyn. **89**, 1569–1578 (2017)
11. Gosak, M., Markovič, R., Dolenšek, J., Rupnik, M.S., Marhl, M., Stožer, A., Perc, M.: Network science of biological systems at different scales: a review. Phys. Life Rev. **24**, 118–135 (2018)
12. Gosak, M., Markovič, R., Dolenšek, J., Rupnik, M.S., Marhl, M., Stožer, A., Perc, M.: Loosening the shackles of scientific disciplines with network science: reply to comments on network science of biological systems at different scales: a review. Phys. Life Rev. **24**, 162–167 (2018)
13. Milton, J., Jung, P.: Epilepsy as a Dynamic Disease. Springer, Berlin (2013)
14. Xu, Y., Jia, Y., Ma, J., Hayat, T., Alsaedi, A.: Collective responses in electrical activities of neurons under field coupling. Sci. Rep. **8**, 1349 (2018)
15. Wang, C., Ma, J.: A review and guidance for pattern selection in spatiotemporal system. Int. J. Mod. Phys. B **32**, 1830003 (2018)
16. Mvogo, A., Takembo, C.N., Fouda, H.P.E., Kofané, T.C.: Pattern formation in diffusive excitable systems under magnetic flow effects. Phys. Lett. A **381**, 2264–2271 (2017)
17. Takembo, C.N., Mvogo, A., Ekobena Fouda, H.P., Kofané, T.C.: Modulated wave formation in myocardial cells under electromagnetic radiation. Int. J. Mod. Phys. B **32**, 1850165 (2018)
18. Xiang, W., Huangpu, Y.: Second-order terminal sliding mode controller for a class of chaotic systems with unmatched uncertainties. Commun. Nonlinear Sci. Numer. Simul. **15**, 3241–3247 (2010)
19. Sinha, S., Sridhar, S.: Patterns in Excitable Media: Genesis, Dynamics, and Control. CRC Press, Boca Raton (2014)
20. Zhang, J., Tang, J., Ma, J., Luo, J.M., Yang, X.Q.: The dynamics of spiral tip adjacent to inhomogeneity in cardiac tissue. Physica A **491**, 340–346 (2018)
21. Banerjee, M., Ghorai, S., Mukherjee, N.: Approximated spiral and target patterns in Bazykins prey-predator model: Multiscale perturbation analysis. Int. J. Bifurc. Chaos **27**, 1750038 (2017)
22. Woo, S.-J., Lee, J., Lee, K.J.: Spiral waves in a coupled network of sine-circle maps. Phys. Rev. E **68**, 016208 (2003)
23. Hu, B., Ma, J., Tang, J.: Selection of multiarmed spiral waves in a regular network of neurons. PLoS ONE **8**, e69251 (2013)
24. Li, F., Ma, J.: Pattern selection in network of coupled multiscroll attractors. PLoS ONE **11**(4), e0154282 (2016)

25. Perc, M.: Effects of small-world connectivity on noise-induced temporal and spatial order in neural media. Chaos Solitons Fractals **31**, 280–291 (2007)
26. Panfilov, A.V., Müller, S.C., Zykov, V.S., Keener, J.P.: Elimination of spiral waves in cardiac tissue by multiple electrical shocks. Phys. Rev. E **61**, 4644–4647 (2000)
27. Pertsov, A.M., Davidenko, J.M., Salomonsz, R., Baxter, W.T., Jalife, J.: Spiral waves of excitation underlie reentrant activity in isolated cardiac muscle. Circ. Res. **72**, 631–650 (1993)
28. Cherry, E.M., Fenton, F.H., Krogh-Madsen, T., Luther, S., Parlitz, U.: Introduction to focus issue complex cardiac dynamics (2017)
29. Cherry, E.M., Fenton, F.H.: Visualization of spiral and scroll waves in simulated and experimental cardiac tissue. New J. Phys. **10**, 125016 (2008)
30. Christini, D.J., Glass, L.: Introduction: mapping and control of complex cardiac arrhythmias. Chaos **12**, 732–739 (2002)
31. Gray, R.A., Pertsov, A.M., Jalife, J.: Spatial and temporal organization during cardiac fibrillation. Nature **392**, 75 (1998)
32. Takagaki, K., Zhang, C., Wu, J.-Y., Ohl, F.W.: Flow detection of propagating waves with temporospatial correlation of activity. J. Neurosci. Methods **200**, 207–218 (2011)
33. Schiff, S.J., Huang, X., Wu, J.-Y.: Dynamical evolution of spatiotemporal patterns in mammalian middle cortex. BMC Neurosci. **8**, P61 (2007)
34. Li, Y., Oku, M., He, G., Aihara, K.: Elimination of spiral waves in a locally connected chaotic neural network by a dynamic phase space constraint. Neural Netw. **88**, 9–21 (2017)
35. Ge, M., Jia, Y., Xu, Y., Yang, L.: Mode transition in electrical activities of neuron driven by high and low frequency stimulus in the presence of electromagnetic induction and radiation. Nonlinear Dyn. **91**, 515–523 (2018)
36. Li, J., Liu, S., Liu, W., Yu, Y., Wu, Y.: Suppression of firing activities in neuron and neurons of network induced by electromagnetic radiation. Nonlinear Dyn. **83**, 801–810 (2016)
37. Wu, F., Wang, C., Xu, Y., Ma, J.: Model of electrical activity in cardiac tissue under electromagnetic induction. Sci. Rep. **6**, 28 (2016)
38. Lv, M., Ma, J.: Multiple modes of electrical activities in a new neuron model under electromagnetic radiation. Neurocomputing **205**, 375–381 (2016)
39. Ma, J., Mi, L., Zhou, P., Xu, Y., Hayat, T.: Phase synchronization between two neurons induced by coupling of electromagnetic field. Appl. Math. Comput. **307**, 321–328 (2017)
40. Perez-Olivas, H., Cordova-Fraga, T., Gómez-Aguilar, F., Rosas-Padilla, E., Lopez-Briones, S., Espinoza-García, A., Villagómez-Castro, J., Bernal-Alvarado, J., Sosa-Aquino, M.: Magnetic exposure system to stimulate human lymphocytes proliferation. In: AIP Conference Proceedings, Volume 1494, pp. 146–148. AIP (2012)
41. Rastogi, P., Lee, E., Hadimani, R.L., Jiles, D.C.: Transcranial magnetic stimulation-coil design with improved focality. AIP Adv. **7**, 056705 (2017)
42. Hindmarsh, J., Rose, R.: A model of the nerve impulse using two first-order differential equations. Nature **296**, 162 (1982)
43. Hodgkin, A.L., Huxley, A.F.: A quantitative description of membrane current and its application to conduction and excitation in nerve. J. Physiol. **117**, 500–544 (1952)
44. Wu, J., Xu, Y., Ma, J.: Lévy noise improves the electrical activity in a neuron under electromagnetic radiation. PLoS ONE **12**, e0174330 (2017)
45. Lv, M., Wang, C., Ren, G., Ma, J., Song, X.: Model of electrical activity in a neuron under magnetic flow effect. Nonlinear Dyn. **85**, 1479–1490 (2016)
46. Chua, L.: Memristor-the missing circuit element. IEEE Trans. Circuit Theory **18**, 507–519 (1971)
47. Li, X., Rakkiyappan, R., Velmurugan, G.: Dissipativity analysis of memristor-based complex-valued neural networks with time-varying delays. Inf. Sci. **294**, 645–665 (2015)
48. Strukov, D.B., Snider, G.S., Stewart, D.R., Williams, R.S.: The missing memristor found. Nature **453**, 80 (2008)
49. Rakkiyappan, R., Sivasamy, R., Li, X.: Synchronization of identical and nonidentical memristor-based chaotic systems via active backstepping control technique. Circuits Syst. Signal Process. **34**, 763–778 (2015)
50. Kandel, E.R., Schwartz, J.H., Jessell, T.M., Siegelbaum, S.A., Hudspeth, A.J., et al.: Principles of Neural Science, vol. 4. McGraw-Hill, New York (2000)
51. Shu, Y., Duque, A., Yu, Y., Haider, B., McCormick, D.A.: Properties of action-potential initiation in neocortical pyramidal cells: evidence from whole cell axon recordings. J. Neurophysiol. **97**, 746–760 (2007)